

Stress and Strain in Perovskite/Silicon Tandem Solar Cells

Cite as

Nano-Micro Lett.
(2023) 15:59

Kong Liu^{1,2} ✉, Zhijie Wang^{1,2}, Shengchun Qu^{1,2}, Liming Ding³ ✉

Received: 30 November 2022
Accepted: 31 January 2023
© The Author(s) 2023

Tandem solar cells based on metal halide perovskites are advancing rapidly during last few years [1–17]. The certified power conversion efficiency (PCE) for monolithic perovskite/silicon tandem solar cell reaches 32.5% [18]. Since tandem solar cells contain more layers than single-junction solar cells, stress/strain control is an issue during fabrication and further practical operation. The stress can not only affect the stability of the perovskite layer but also change the optoelectronic properties of the films [19–23].

The mismatch for thermal expansion coefficients or lattice constants induces the stress in stacked films. However, a variety of organic and inorganic materials with different thermal expansion coefficients and lattice constants are needed in perovskite/silicon tandem solar cells. The thermal expansion coefficients for perovskite and organic layers are generally one order of magnitude higher than transparent conductive oxide (TCO) films and glass substrate [19, 24]. Several stimuli can induce compressive or tensile stress in films. For example, residual stress can form during physical deposition and thermal annealing of the perovskite film. Additionally, when the device is applied in a practical environment, the temperature change or external force can form stress in the films [25]. The following equation presents the relationship between stress ($\sigma_{\Delta T}$) and temperature changes (ΔT) [19]:

$$\sigma_{\Delta T} = \frac{E_f}{1 - \nu_f} (a_s - a_f) \Delta T \quad (1)$$

where E_f and ν_f are the Young's modulus and Poisson's ratio for the films; a_f and a_s are the thermal expansion coefficients

for the films and the substrate. The typical E_f , ν_f and thermal expansion coefficient of perovskite are 20.5 GPa, 0.33 and $6.1 \times 10^{-5} \text{ K}^{-1}$, respectively, and the typical thermal expansion coefficient of glass is $3.7 \times 10^{-6} \text{ K}^{-1}$ [19, 24]. If the temperature decreases from 80 to 30 °C, a tensile stress of 87.66 MPa can form in perovskite film.

Stress in films can cause problems in perovskite/silicon tandem solar cells. If the stress is strong enough, the structure of the tandem device may be destroyed. For the perovskite layer, the compressive stresses greater than the critical stress (σ_c) can cause layer failure or delamination (Fig. 1a, b) [19, 26, 27]. Moreover, the strain in the perovskite layer may result in stress in adjacent layers [28]. The sputtered indium zinc oxide (IZO) electrode on perovskite/silicon tandem solar cell surface exhibited peeling-off or wrinkling due to the strong stress induced by the bombardment of sputtered high-energy particles (Fig. 1c) [29]. Notably, the perovskite film coated on glass showed less strain than the perovskite film coated on indium tin oxide (ITO)/glass, which could be attributed to different bonding strengths between the perovskite and substrates due to different roughness of ITO and glass surface [24]. The wrinkled IZO electrode can form under compressive stress induced by strain in the perovskite layer. To mitigate the stresses and overcome film delamination, some methods were adopted, e.g., using a buffer layer with better affinity (Fig. 1d), matching lattice constants and thermal expansion coefficients for the films, or reducing the particle energy and substrate temperature during physical

✉ Kong Liu, liukong@semi.ac.cn; Liming Ding, ding@nanoctr.cn

¹ Key Laboratory of Semiconductor Materials Science (CAS), Beijing Key Laboratory of Low Dimensional Semiconductor Materials and Devices, Institute of Semiconductors, Chinese Academy of Sciences, Beijing 100083, People's Republic of China

² Center of Materials Science and Optoelectronics Engineering, University of Chinese Academy of Sciences, Beijing 100049, People's Republic of China

³ Center for Excellence in Nanoscience (CAS), Key Laboratory of Nanosystem and Hierarchical Fabrication (CAS), National Center for Nanoscience and Technology, Beijing 100190, People's Republic of China



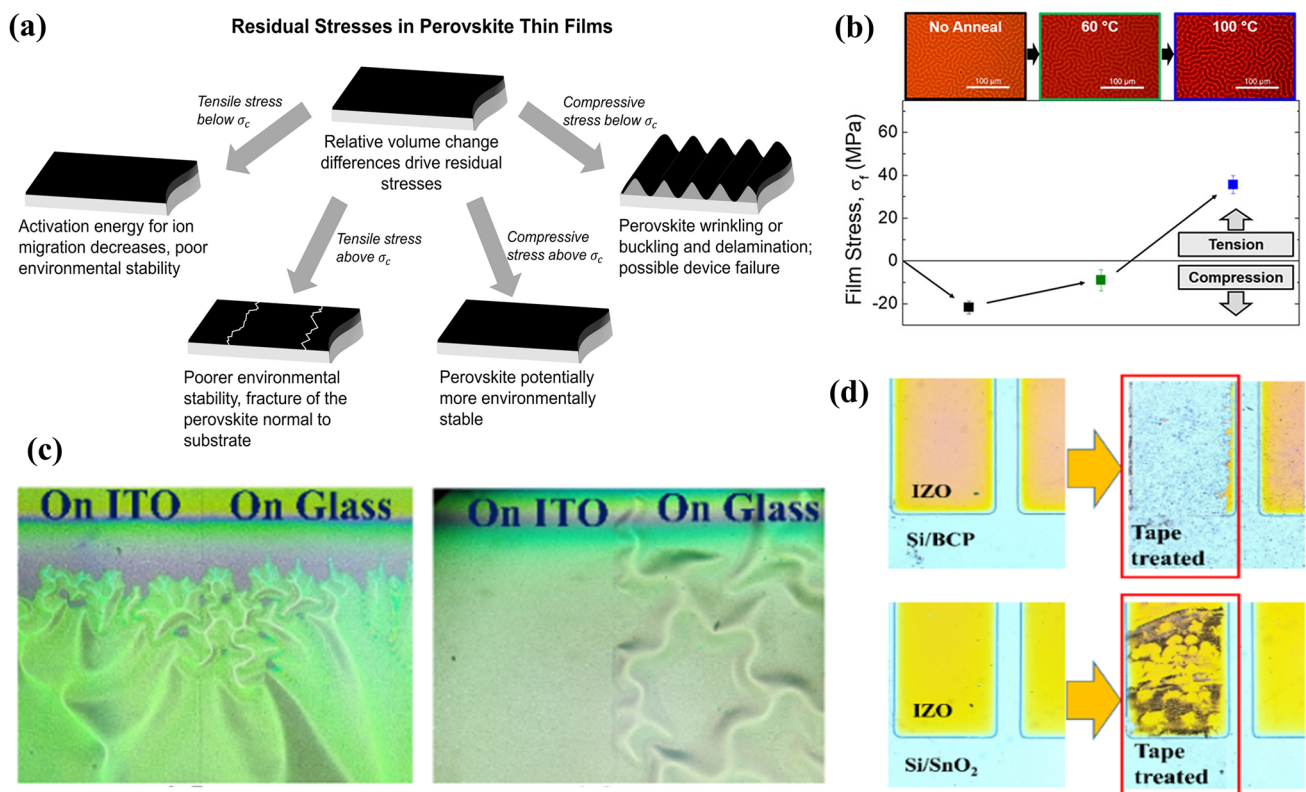


Fig. 1 **a** Schematic for stresses and their effects on perovskite films. Reproduced with permission [19], Copyright 2021, American Chemical Society. **b** Wrinkled perovskite film induced by strong compressive stress. Reproduced with permission [26], Copyright 2018, American Chemical Society. **c** Wrinkled IZO film induced by compressive stress transmitted from perovskite layer. **d** IZO films treated by tape, demonstrating that SnO₂ has better affinity with IZO than BCP. Reproduced with permission [29], Copyright 2022, The Royal Society of Chemistry

deposition [30]. Encapsulation can help to mitigate stress-induced harm to the devices [31].

Even if stress does not cause peeling-off or wrinkling, it may cause other results. In general, moderate stress can cause dislocations or defects at the interface, leading to enhanced recombination of photogenerated carriers. At the same time, the stress can facilitate light-induced phase segregation of wide-bandgap perovskite or vary the lattice structure of the perovskite directly, leading to bandgap change (Fig. 2a) [22, 31–38]. Wang et al. [39] modulated strain in perovskite/silicon tandem solar cells by adding adenosine triphosphate (ATP) (Fig. 2b). Owing to the enhanced energy barrier for ion migration and reduced light-induced phase segregation in wide-bandgap perovskite, the devices exhibited a remarkable long-term operational stability, keeping 83.60% of the initial PCE after 2500 h. Chen et al. [40] found that the photoluminescence (PL) peak of the perovskite film on silicon exhibited blue shift compared with that

on glass substrate (Fig. 2c). Different substrates cause different levels of lattice mismatching between the perovskite and the substrates, leading to different stress and bandgap in perovskite. Because the bandgap of the absorber is a significant factor influencing current matching between sub-cells, such bandgap changes should be noted when investigating single-junction perovskite solar cells on a glass substrate while tandem solar cells on silicon bottom cells.

A possible strategy to reduce the stresses in tandem solar cells is that the films in top cells are formed in a nonplanar structure rather than planar structure. Because stress accumulation can occur more easily in a planar film than in a nonplanar structure. Fortunately, the surface of silicon bottom cells can be textured and served as a light-trapping structure, which provides a foundation for nonplanar structuring. However, most textured structures have sharp edges and corners, which do not facilitate thin film formation. In addition, such structures may lead to the formation of spots

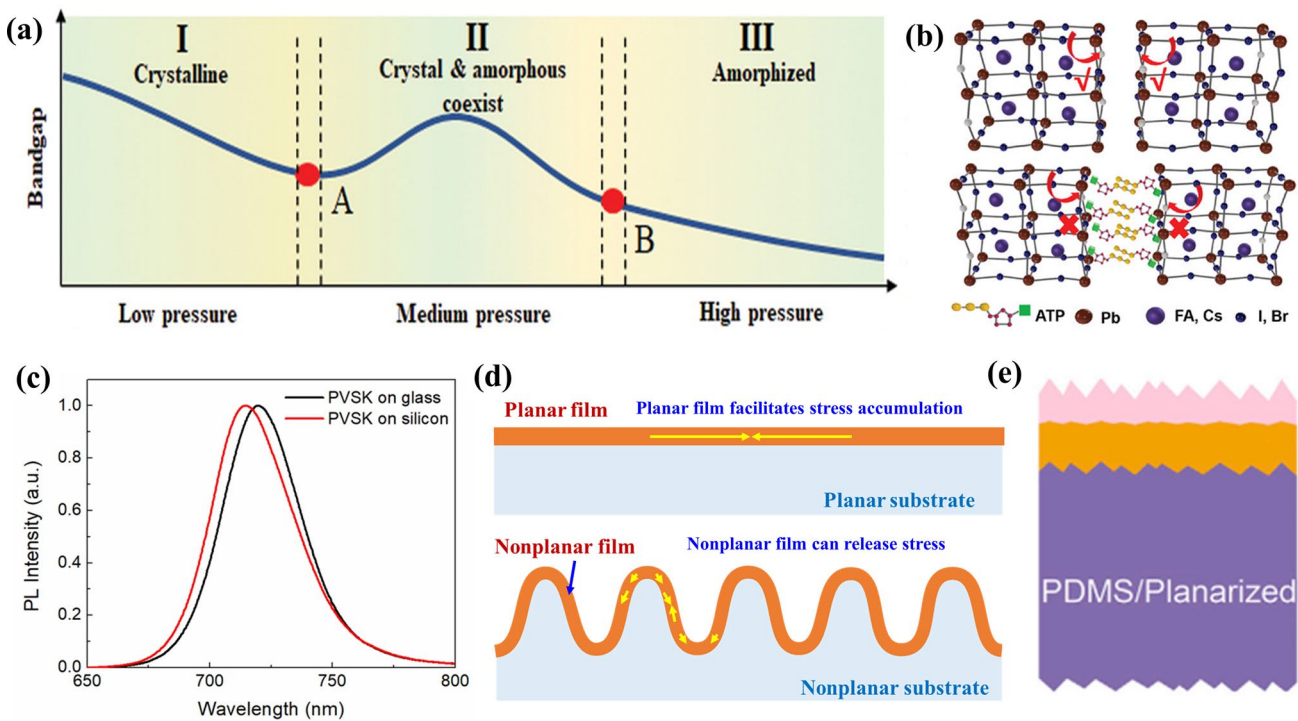


Fig. 2 **a** Stress changes the bandgap of perovskites. Reproduced with permission [22], Copyright 2020, Wiley–VCH. **b** Strain reduction in perovskite by introducing ATP. Reproduced with permission [39], Copyright 2022, Wiley–VCH. **c** PL for perovskites on glass and silicon substrates. Reproduced with permission [40], Copyright 2018, Elsevier. **d** Nonplanar structure for stress relaxation in films. **e** Nonplanar silicon top surface can facilitate doctor blading of large-area perovskite films. Reproduced with permission [44], Copyright 2020, Elsevier

with large local stress or defects. Therefore, a nonplanar light-trapping structure without sharp edges and corners may be needed in future perovskite/silicon tandem solar cells [41–43]. As exhibited in Fig. 2d, after introducing such structure, the stress in the films can be relaxed easily even if the device is undergoing external force impact. A textured structure with smoothed edges and corners can realize large-area perovskite film fabrication via doctor blading method (Fig. 2e) [44].

Perovskite itself can form local stress/strain in its lattice. Goldschmidt tolerance factor (t), $(R_A + R_X)/[\sqrt{2}(R_B + R_X)]$, is used to evaluate the crystal structure of perovskites [19, 23], where R_A , R_X , and R_B are the radius of ions at A, X, and B positions of perovskites (ABX_3). An ideal cubic structure can be formed when $0.8 < t < 1$. For certain B and X ions, A cation should have a proper size; otherwise, large strain will be formed in the lattice, resulting in phase transition or instability of perovskite films. For perovskites with $APbI_3$ structure, A position can be MA^+ ($CH_3NH_3^+$, $t=0.83$) or FA^+ ($(NH_2)_2CH^+$, $t=0.99$). However, FA^+ has a larger size

than MA^+ , which will lead to a larger size mismatch and local lattice strain. To relax stress in $FAPbI_3$ and stabilize the lattice, some small ions, e.g., MA^+ , Rb^+ , or Cs^+ , are incorporated in A position [19, 22, 45–47].

In short, the stress and strain are issues in developing perovskite/silicon tandem solar cells. The issues become severe when the device area is enlarged, causing current mismatch in the sub-cells. Strategies should be proposed to solve these issues.

Acknowledgements The authors appreciate the National Key Research and Development Program of China (2018YFE0204000), the Strategic Priority Research Program of the Chinese Academy of Sciences (XDB43000000), the National Natural Science Foundation of China (62274155, U20A20206, 51972300 and 21975245). K. Liu thanks the Youth Innovation Promotion Association (CAS) (2020114), and the Beijing Nova Program (2020117). L. Ding thanks the National Key Research and Development Program of China (2022YFB3803300), the open research fund of Songshan Lake Materials Laboratory (2021SLABFK02), and the National Natural Science Foundation of China (21961160720).

Open Access This article is licensed under a Creative Commons Attribution 4.0 International License, which permits use, sharing, adaptation, distribution and reproduction in any medium or format, as long as you give appropriate credit to the original author(s) and the source, provide a link to the Creative Commons licence, and indicate if changes were made. The images or other third party material in this article are included in the article's Creative Commons licence, unless indicated otherwise in a credit line to the material. If material is not included in the article's Creative Commons licence and your intended use is not permitted by statutory regulation or exceeds the permitted use, you will need to obtain permission directly from the copyright holder. To view a copy of this licence, visit <http://creativecommons.org/licenses/by/4.0/>.

References

1. K.A. Bush, A.F. Palmstrom, Z.S.J. Yu, M. Boccard, R. Cheacharoen et al., 23.6%-efficient monolithic perovskite/silicon tandem solar cells with improved stability. *Nat. Energy* **2**(4), 17009 (2017). <https://doi.org/10.1038/nenergy.2017.9>
2. F. Sahli, J. Werner, B.A. Kamino, M. Brauning, R. Monnard et al., Fully textured monolithic perovskite/silicon tandem solar cells with 25.2% power conversion efficiency. *Nat. Mater.* **17**(9), 820–826 (2018). <https://doi.org/10.1038/s41563-018-0115-4>
3. A. Al-Ashouri, E. Kohnen, B. Li, A. Magomedov, H. Hempel et al., Monolithic perovskite/silicon tandem solar cell with > 29% efficiency by enhanced hole extraction. *Science* **370**(6522), 1300–1309 (2020). <https://doi.org/10.1126/science.abd4016>
4. Y. Hou, E. Aydin, M. De Bastiani, C.X. Xiao, F.H. Isikgor et al., Efficient tandem solar cells with solution-processed perovskite on textured crystalline silicon. *Science* **367**(6482), 1135–1140 (2020). <https://doi.org/10.1126/science.aaz3691>
5. D. Kim, H.J. Jung, I.J. Park, B.W. Larson, S.P. Dunfield et al., Efficient, stable silicon tandem cells enabled by anion-engineered wide-bandgap perovskites. *Science* **368**(6487), 155–160 (2020). <https://doi.org/10.1126/science.aba3433>
6. J. Liu, M. De Bastiani, E. Aydin, G.T. Harrison, Y.J. Gao et al., Efficient and stable perovskite-silicon tandem solar cells through contact displacement by MgF_x . *Science* **377**(6603), 302–306 (2022). <https://doi.org/10.1126/science.abn8910>
7. D.P. McMeekin, G. Sadoughi, W. Rehman, G.E. Eperon, M. Saliba et al., A mixed-cation lead mixed-halide perovskite absorber for tandem solar cells. *Science* **351**(6269), 151–155 (2016). <https://doi.org/10.1126/science.aad5845>
8. J.X. Xu, C.C. Boyd, Z.S.J. Yu, A.F. Palmstrom, D.J. Witter et al., Triple-halide wide-band gap perovskites with suppressed phase segregation for efficient tandems. *Science* **367**(6482), 1097–1104 (2020). <https://doi.org/10.1126/science.aaz5074>
9. L. Mazzarella, Y.H. Lin, S. Kirner, A.B. Morales-Vilches, L. Korte et al., Infrared light management using a nanocrystalline silicon oxide interlayer in monolithic perovskite/silicon heterojunction tandem solar cells with efficiency above 25%. *Adv. Energy Mater.* **9**(14), 1803241 (2019). <https://doi.org/10.1002/aenm.201803241>
10. L. Liu, Z. Xiao, C. Zuo, L. Ding, Inorganic perovskite/organic tandem solar cells with efficiency over 20%. *J. Semicond.* **42**(2), 020501 (2021). <https://doi.org/10.1088/1674-4926/42/2/020501>
11. J. Sun, L. Ding, Perovskite/organic tandem solar cells. *J. Semicond.* **44**(2), 020201 (2023). <https://doi.org/10.1088/1674-4926/44/2/020201>
12. L. Liu, H. Xiao, K. Jin, Z. Xiao, X. Du et al., 4-terminal inorganic perovskite/organic tandem solar cells offer 22% efficiency. *Nano-Micro Lett.* **15**(1), 23 (2022). <https://doi.org/10.1007/s40820-022-00995-2>
13. S. Chen, C. Zuo, B. Xu, L. Ding, Monolithic perovskite/silicon tandem solar cells offer an efficiency over 29%. *J. Semicond.* **42**(12), 120203 (2021). <https://doi.org/10.1088/1674-4926/42/12/120203>
14. Y. Cheng, L. Ding, Perovskite/Si tandem solar cells: fundamentals, advances, challenges, and novel applications. *SusMat* **1**(3), 324–344 (2021). <https://doi.org/10.1002/sus2.25>
15. Z. Fang, Q. Zeng, C. Zuo, L. Zhang, H. Xiao et al., Perovskite-based tandem solar cells. *Sci. Bull.* **66**(6), 621–636 (2021). <https://doi.org/10.1016/j.scib.2020.11.006>
16. D. Zhao, L. Ding, All-perovskite tandem structures shed light on thin-film photovoltaics. *Sci. Bull.* **65**(14), 1144–1146 (2020). <https://doi.org/10.1016/j.scib.2020.04.013>
17. Q. Zeng, L. Liu, Z. Xiao, F. Liu, Y. Hua et al., A two-terminal all-inorganic perovskite/organic tandem solar cell. *Sci. Bull.* **64**(13), 885–887 (2019). <https://doi.org/10.1016/j.scib.2019.05.015>
18. NREL, "Best Research-cell Efficiency Chart," www.nrel.gov/pv/cell-efficiency.html Accessed: 20 Dec 2022
19. M. Dailey, Y.N. Li, A.D. Printz, Residual film stresses in perovskite solar cells: origins, effects, and mitigation strategies. *ACS Omega* **6**(45), 30214–30223 (2021). <https://doi.org/10.1021/acsomega.1c04814>
20. H. Zhang, N.G. Park, Strain control to stabilize perovskite solar cells. *Angew. Chem. Int. Ed.* **61**(48), e202212268 (2022). <https://doi.org/10.1002/anie.202212268>
21. B.W. Yang, D. Bogachuk, J.J. Suo, L. Wagner, H. Kim et al., Strain effects on halide perovskite solar cells. *Chem. Soc. Rev.* **51**(17), 7509–7530 (2022). <https://doi.org/10.1039/d2cs00278g>
22. Y.A. Jiao, S.H. Yi, H.W. Wang, B. Li, W.Z. Hao et al., Strain engineering of metal halide perovskites on coupling anisotropic behaviors. *Adv. Funct. Mater.* **31**(4), 202006243 (2021). <https://doi.org/10.1002/adfm.202006243>
23. J.P. Wu, S.C. Liu, Z.B. Li, S. Wang, D.J. Xue et al., Strain in perovskite solar cells: origins, impacts and regulation. *Natl. Sci. Rev.* **8**(8), nwab047 (2021). <https://doi.org/10.1093/nsr/nwab047>
24. J.J. Zhao, Y.H. Deng, H.T. Wei, X.P. Zheng, Z.H. Yu et al., Strained hybrid perovskite thin films and their impact on the

- intrinsic stability of perovskite solar cells. *Sci. Adv.* **3**(11), eaa05616 (2017). <https://doi.org/10.1126/sciadv.aao5616>
25. B. Chen, T. Li, Q.F. Dong, E. Mosconi, J.F. Song et al., Large electrostrictive response in lead halide perovskites. *Nat. Mater.* **17**(11), 1020–1026 (2018). <https://doi.org/10.1038/s41563-018-0170-x>
 26. K.A. Bush, N. Rolston, A. Gold-Parker, S. Manzoor, J. Hausele et al., Controlling thin-film stress and wrinkling during perovskite film formation. *ACS Energy Lett.* **3**(6), 1225–1232 (2018). <https://doi.org/10.1021/acseenergylett.8b00544>
 27. W. Zhu, L. Yang, J.W. Guo, Y.C. Zhou, C. Lu, Numerical study on interaction of surface cracking and interfacial delamination in thermal barrier coatings under tension. *Appl. Surf. Sci.* **315**, 292–298 (2014). <https://doi.org/10.1016/j.apsusc.2014.07.142>
 28. S.G. Kim, J.H. Kim, P. Ramming, Y. Zhong, K. Schotz et al., How antisolvent miscibility affects perovskite film wrinkling and photovoltaic properties. *Nat. Commun.* **12**(1), 1554 (2021). <https://doi.org/10.1038/s41467-021-21803-2>
 29. K. Liu, B. Chen, Z.S.J. Yu, Y.L. Wu, Z.T. Huang et al., Reducing sputter induced stress and damage for efficient perovskite/silicon tandem solar cells. *J. Mater. Chem. A* **10**(3), 1343–1349 (2022). <https://doi.org/10.1039/d1ta09143c>
 30. M.D. Thouless, Cracking and delamination of coatings. *J. Vac. Sci. Technol. A* **9**(4), 2510–2515 (1991). <https://doi.org/10.1116/1.577265>
 31. C.C. Boyd, R. Checharoen, T. Leijtens, M.D. McGehee, Understanding degradation mechanisms and improving stability of perovskite photovoltaics. *Chem. Rev.* **119**(5), 3418–3451 (2019). <https://doi.org/10.1021/acs.chemrev.8b00336>
 32. Q. Li, S.R. Li, K. Wang, Z.W. Quan, Y. Meng et al., High-pressure study of perovskite-like organometal halide: band-gap narrowing and structural evolution of $[\text{NH}_3(\text{CH}_2)_4\text{NH}_3]\text{CuCl}_4$. *J. Phys. Chem. Lett.* **8**(2), 500–506 (2017). <https://doi.org/10.1021/acs.jpcclett.6b02786>
 33. C.Y. Ge, M.Y. Hu, P. Wu, Q. Tan, Z.Z. Chen et al., Ultralow thermal conductivity and ultrahigh thermal expansion of single-crystal organic-inorganic hybrid perovskite $\text{CH}_3\text{NH}_3\text{PbX}_3$ ($X = \text{Cl}, \text{Br}, \text{I}$). *J. Phys. Chem. C* **122**(28), 15973–15978 (2018). <https://doi.org/10.1021/acs.jpcc.8b05919>
 34. D.J. Xue, Y. Hou, S.C. Liu, M.Y. Wei, B. Chen et al., Regulating strain in perovskite thin films through charge-transport layers. *Nat. Commun.* **11**(1), 1514 (2020). <https://doi.org/10.1038/s41467-020-15338-1>
 35. Y.C. Zhao, P. Miao, J. Elia, H.Y. Hu, X.X. Wang et al., Strain-activated light-induced halide segregation in mixed-halide perovskite solids. *Nat. Commun.* **11**(1), 6328 (2020). <https://doi.org/10.1038/s41467-020-20066-7>
 36. A. Ummadisingu, S. Meloni, A. Mattoni, W. Tress, M. Gratzel, Crystal-size-induced band gap tuning in perovskite films. *Angew. Chem. Int. Ed.* **60**(39), 21368–21376 (2021). <https://doi.org/10.1002/anie.202106394>
 37. M.R. Islam, A.S.M.J. Islam, K. Liu, Z.J. Wang, S.C. Qu et al., Strain-induced tunability of the optoelectronic properties of inorganic lead iodide perovskites APbI_3 ($A = \text{Rb}$ and Cs). *Physica B* **638**, 413960 (2022). <https://doi.org/10.1016/j.physb.2022.413960>
 38. R. Islam, K. Liu, Z.J. Wang, S. Hasan, Y.L. Wu et al., Strain-induced electronic and optical properties of inorganic lead halide perovskites APbBr_3 ($A = \text{Rb}$ and Cs). *Mater. Today Commun.* **31**, 103305 (2022). <https://doi.org/10.1016/j.mtcomm.2022.103305>
 39. L.N. Wang, Q.Z. Song, F.T. Pei, Y.H. Chen, J. Dou et al., Strain modulation for light-stable n-i-p perovskite/silicon tandem solar cells. *Adv. Mater.* **34**(26), 202201315 (2022). <https://doi.org/10.1002/adma.202201315>
 40. B. Chen, Z.S. Yu, K. Liu, X.P. Zheng, Y. Liu et al., Grain engineering for perovskite/silicon monolithic tandem solar cells with efficiency of 25.4%. *Joule* **3**(1), 177–190 (2019). <https://doi.org/10.1016/j.joule.2018.10.003>
 41. K. Mantulnikovs, A. Glushkova, P. Matus, L. Ciric, M. Kollar et al., Morphology and photoluminescence of $\text{CH}_3\text{NH}_3\text{PbI}_3$ deposits on nonplanar, strongly curved substrates. *ACS Photonics* **5**(4), 1476–1485 (2018). <https://doi.org/10.1021/acsp Photonics.7b01496>
 42. K. Liu, Y. Sun, Q.C. Li, C. Yang, M. Azam et al., A wrinkled structure with broadband and omnidirectional light-trapping abilities for improving the performance of organic solar cells with low defect density. *Nanoscale* **11**(46), 22467–22474 (2019). <https://doi.org/10.1039/c9nr08477k>
 43. P. Tockhorn, J. Sutter, A. Cruz, P. Wagner, K. Jäger et al., Nano-optical designs for high-efficiency monolithic perovskite–silicon tandem solar cells. *Nat. Nanotechnol.* **17**(11), 1214–1221 (2022). <https://doi.org/10.1038/s41565-022-01228-8>
 44. B. Chen, Z.S.J. Yu, S. Manzoor, S. Wang, W. Weigand et al., Blade-coated perovskites on textured silicon for 26%-efficient monolithic perovskite/silicon tandem solar cells. *Joule* **4**(4), 850–864 (2020). <https://doi.org/10.1016/j.joule.2020.01.008>
 45. Y.Y. Zhao, J.L. Duan, Y.D. Wang, X.Y. Yang, Q.W. Tang, Precise stress control of inorganic perovskite films for carbon-based solar cells with an ultrahigh voltage of 1.622 V. *Nano Energy* **67**, 104286 (2020). <https://doi.org/10.1016/j.nanoen.2019.104286>
 46. M. Ross, S. Severin, M.B. Stutz, P. Wagner, H. Kobler et al., Co-evaporated formamidinium lead iodide based perovskites with 1000 h constant stability for fully textured monolithic perovskite/silicon tandem solar cells. *Adv. Energy Mater.* **11**(35), 2101460 (2021). <https://doi.org/10.1002/aenm.202101460>
 47. J.Z. Jiang, M. Xiong, K. Fan, C.X. Bao, D.Y. Xin et al., Synergistic strain engineering of perovskite single crystals for highly stable and sensitive X-ray detectors with low-bias imaging and monitoring. *Nat. Photonics* **16**(8), 575–581 (2022). <https://doi.org/10.1038/s41566-022-01024-9>

